NASA/CR-2000-210298

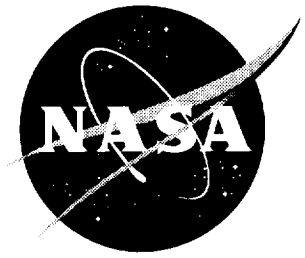

An Estimation of Turbulent Kinetic Energy and Energy Dissipation Rate Based on Atmospheric Boundary Layer Similarity Theory

Jongil Han, S. Pal Arya, Shaohua Shen, and Yuh-Lang Lin
North Carolina State University, Raleigh, North Carolina

National Aeronautics and
Space Administration

Langley Research Center
Hampton, Virginia 23681-2199

Prepared for Langley Research Center
under Cooperative Agreement NCC1-188

June 2000

Available from:

NASA Center for AeroSpace Information (CASI)
7121 Standard Drive
Hanover, MD 21076-1320
(301) 621-0390

National Technical Information Service (NTIS)
5285 Port Royal Road
Springfield, VA 22161-2171
(703) 605-6000

Abstract

Algorithms are developed to extract atmospheric boundary layer profiles for turbulence kinetic energy (TKE) and energy dissipation rate (EDR), with data from a meteorological tower as input. The profiles are based on similarity theory and scalings for the atmospheric boundary layer. The calculated profiles of EDR and TKE are required to match the observed values at 5 and 40 m. The algorithms are coded for operational use and yield plausible profiles over the diurnal variation of the atmospheric boundary layer.

Contents

List of Tables

List of Figures

Nomenclature

e = turbulence kinetic energy
f = Coriolis parameter
g = gravitational acceleration
h = height of atmospheric boundary layer
L = Obukhov length
k = von Karman constant, 0.4
Ri = gradient Richardson number
T_0 = reference temperature
$\bar{u}$ = mean velocity in the direction of the wind
u_* = friction velocity
u', v' = horizontal velocity fluctuations
w_* = convective velocity scale
w' = vertical velocity fluctuation
z = elevation above the ground
ϵ = turbulent kinetic energy dissipation rate
ζ = Monin-Obukhov stability parameter, z/L
$\bar{\theta_v}$ = mean virtual potential temperature
$\theta_v{}'$ = virtual potential temperature fluctuation
ϕ_h = dimensionless potential temperature gradient in the surface layer
ϕ_m = dimensionless wind shear in the surface layer

1 Introduction

To safely reduce aircraft spacing and increase airport capacity, NASA is developing a predictor system, called the Aircraft VOrtex Spacing System (AVOSS: Hinton, 1995; Hinton et al., 1999; Perry et al., 1997). This system includes prediction algorithms for aircraft wake vortex transport and decay. Semi-empirical vortex prediction algorithms have been developed and incorporated within the AVOSS (Robins et al., 1998; Sarpkaya et al., 2000). One of the key input elements for the AVOSS prediction algorithms is the atmospheric boundary layer (ABL) turbulence of which the intensity can be represented by turbulent kinetic energy (TKE) or eddy energy dissipation rate (EDR). While the prediction algorithms require the vertical profiles for the TKE and EDR at least up to the vortex generation height, the observational data for the TKE and EDR are available only from a meteorological tower at the heights of 5 and 40 m above the ground.

In supporting the NASA AVOSS project, the wake vortex research group at North Carolina State University (NCSU) has developed algorithms and software which can generate the vertical profiles of TKE and EDR. These algorithms are based on the ABL similarity relations (Arya, 1988, 1995, 2000; Caughey et al., 1979; Rao and Nappo, 1998; Sorbjan, 1989; Stull, 1988) and available experimental data.

Section 2 describes the ABL similarity relations with respect to the vertical profiles of the TKE and EDR that are dependent upon the ABL stability. Section 3 contains a detailed description of the software. In Section 4, estimates from the similarity relations are compared with the observed data. Section 5 provides information on running the software. Finally, the summary of this study is given in Section 6.

2 Similarity Relations for the TKE and EDR Profiles

ABL observations frequently show consistent and repeatable characteristics from which empirical similarity relationships have been obtained for the variables of interest such as TKE and EDR. Similarity theory is based on the organization of variables into dimensionless groups that come out of the dimensional analysis. The dimensional analysis is a technique used in science and engineering to establish a relationship between different quantities. The functional relationships between dimensionless groups are referred to as similarity relations, because they express the conditions under which two or more flow regimes would be similar. Similarity relationships that have certain universal properties are usually designed to apply to equilibrium (steady-state) situations. One of the well-known similarity relations is the logarithmic velocity profile law observed in surface or wall layers under neutral stratification.

The proposed similarity relationships for TKE and EDR are fundamentally based on the Monin-Obukhov similarity (Monin and Obukhov, 1954) and mixed-layer similarity (Deardorff, 1972) theories. The former is applied to a stratified surface layer and is sometimes called the surface-layer similarity theory, whereas the latter is applied to mixed layers that often develops during daytime convective conditions. These similarity theories have provided the most suitable and acceptable framework for organizing and presenting the ABL data, as well as for extrapolating and predicting certain ABL information where direct measurements of the same are not available.

Using the framework of these similarity theories, a variety of similarity relationships have been suggested to describe the vertical profiles of mean and turbulence fields as functions of the dimensionless groups z/L and/or z/h, covering whole ABL including the surface layer (Arya, 1988, 1995, 2000; Caughey et al., 1979; Hogstrom, 1996; Rao and Nappo, 1998; Sorbjan, 1989; Stull, 1988). Occasionally, various investigators have suggested different values for the empirical coefficients. Based on the similarity scaling in the atmospheric surface layer and boundary layer under different stability conditions, the expressions and parameterizations for the vertical profiles of TKE and EDR and related characteristic scales

are suggested in the following subsections; some of the expressions are adopted directly from those references, whereas the others are derived using the similarity relationships of turbulence variables other than TKE and EDR.

2.1 Neutral and Stable Boundary Layers ($z/L \geq 0$)

The boundary layer may be subdivided into a surface layer (in which stress is nearly constant with height) and an outer layer. A separate set of algorithms is assigned to each sublayer as follows.

2.1.1 Surface Layer ($z \leq 0.1h$)

In the surface layer, the TKE (e) and EDR (ϵ) are given by (Hogstrom, 1996; Rao and Nappo, 1998)

$$e = 6u_*^2, \tag{1}$$

$$\epsilon = \frac{u_*^3}{kz}\left(1.24 + 4.3\frac{z}{L}\right), \tag{2}$$

where $k \simeq 0.4$ is von Karman constant. The friction velocity, u_*, is defined as

$$u_*^2 = \left[\left(\overline{u'w'}\right)_s^2 + \left(\overline{v'w'}\right)_s^2\right]^{1/2}, \tag{3}$$

where the right hand side of *Eq.* (3) represents the total vertical momentum flux near the surface (the subscript s denotes the ground surface). The Obukhov length L depends on both the momentum and heat fluxes near the surface and is defined later; the ratio z/L is the fundamental similarity parameter of the Monin-Obukhov similarity theory.

2.1.2 Outer Layer ($z > 0.1h$)

Expressions for the outer layer can be assigned according to the level of stratification.

(1) Neutral and Stable Boundary Layer

In the neutral and moderately stable boundary layer, the TKE and EDR are given by (Hogstrom, 1996; Rao and Nappo, 1998)

$$\epsilon = 6u_*^2\left(1 - \frac{z}{h}\right)^{1.75}, \tag{4}$$

$$\epsilon = \frac{u_*^3}{kz}\left(1.24 + 4.3\frac{z}{L}\right)\left(1 - 0.85\frac{z}{h}\right)^{1.5}. \tag{5}$$

Alternatively, *Eqs.*(4) and (5) may also be used for the entire boundary layer, including the surface layer.

(2) Very Stable and Decoupled Layers

In the very stable boundary layer and decoupled layers, the TKE and EDR can be expressed by extension of *Eqs.*(1) and (2) as

$$e = 6u_L^2, \tag{6}$$

$$\epsilon = 4.3\frac{u_L^3}{kL_L}, \tag{7}$$

where u_L is the local (friction) velocity scale and L_L is the local buoyancy length scale. Under very stable conditions, the elevated layers of turbulence are decoupled from the surface and the local fluxes and scales cannot be reliably estimated. Perhaps, an empirical relationship between the overall turbulence intensity ($e^{1/2}/\bar{u}$) and Richardson number should be explored. It is worthwhile to note that some experimental results show that *Eq.*(5) can be still used to estimate ϵ even in a very stable boundary layer.

2.2 Unstable Boundary Layer ($z/L < 0$)

The unstable ABL such as during daytime surface heating can be divided into three regimes depending upon the stability parameter, z/L or h/L.

2.2.1 Strongly Unstable (Convective) Regime ($|z/L| > 0.5$)

The structure of the convective regime is dominated by buoyancy. The mean wind velocity and potential temperature profiles are nearly uniform with height. For this reason, the convective outer layer is called the "mixed layer." The mixed layer is topped by an inversion layer in which temperature increases with height. A broad maximum of TKE is usually found in the middle of the mixed layer, while EDR decreases slightly with height.

(1) Surface Layer ($z \leq 0.1h$)

In the surface layer, the TKE and EDR are given by (Arya, 2000)

$$e = 0.36w_*^2 + 0.85u_*^2\left(1 - 3\frac{z}{L}\right)^{2/3}, \tag{8}$$

$$\epsilon = \frac{u_*^3}{kz}\left(1 + 0.5\left|\frac{z}{L}\right|^{2/3}\right)^{3/2}. \tag{9}$$

(2) Mixed Layer

In the mixed layer, the TKE is given by (Arya, 2000)

$$e = \left(0.36 + 0.9\left(\frac{z}{h}\right)^{\frac{2}{3}}\left(1 - 0.8\frac{z}{h}\right)^2\right) w_*^2, \tag{10}$$

or, for most practical purposes,

$$e = 0.54\, w_*^2. \tag{11}$$

The EDR decreases slowly with height at a linear rate (Sorbjan, 1989), i.e.,

$$\epsilon = \frac{w_*^3}{h}\left(0.8 - 0.3\frac{z}{h}\right), \tag{12}$$

where the convective velocity scale w_* is defined as

$$w_* = \left(\frac{g}{T_0}(\overline{w'\theta_v'})_s h\right)^{1/3}. \tag{13}$$

Here g is the gravitational acceleration, T_0 is the reference temperature, and $(\overline{w'\theta_v'})_s$ is the mean surface heat flux.

2.2.2 Moderately Unstable Regime ($0.02 < |z/L| \leq 0.5$)

In this regime, the mechanical production of TKE is comparable with buoyancy production of TKE, i.e., turbulence generation from vertical wind shear is comparable to that generated from surface heating. The TKE in this regime is more or less uniform over the boundary layer or may decrease slightly with height, and the boundary layer structure may be more uncertain.

2.2.3 Weakly Unstable (Near-Neutral) Regime ($|z/L| \leq 0.02$ or $|h/L| \leq 1.5$)

This regime often occurs during the transition period of early morning and late afternoon or during overcast days with strong winds. The lapse rate for temperature tends to be near-neutral. In this regime, mechanical (shear) production dominates the TKE budget.

3 Software Description

In order to generate vertical profiles of TKE and EDR for operational applications, software is written which utilizes the algorithms in the previous section with observations measured at 5 and $40\,m$ above the ground. With the determination of the characteristic similarity scales (such as L, u_*, w_*, and h), the computation of the TKE and EDR profiles is straightforward. The characteristic similarity scales can be estimated from the winds and virtual potential temperatures measured at two levels near the ground.

Since the atmospheric similarity relationships are based on the mean quantities of the observed wind, temperature, and turbulence, the required time averaging interval for EDR and TKE profiles should be at least 30 minutes (Stull, 1988). Hence, with the exception of TKE, all measured variables are 30-minute averaged. For the measured TKE, a 30-minute median value is used, since sporadic measurements of exceptionally large TKE can cause an unrealistic TKE average.

The vertical profiles generated from similarity theory are additionally required to match the measured values at $z = 5$ and $40\,m$ as closely as possible. Often the profiles generated from similarity expressions do not exactly match the observed values at $z = 5$ and $40\,m$ simultaneously. Therefore, the TKE and EDR profiles between $z = 5$ and $40\,m$ are assumed to be linear and independent of the similarity relationships. In addition, upper and lower bounds for the values of TKE and EDR at $z = 5\,m$ are specified to prevent unrealistically large or small values compared with those at $z = 40\,m$. Above $40\,m$, the similarity profiles are used, but are adjusted to match the observed TKE and EDR at $z = 40\,m$.

3.1 Determination of Surface Layer Similarity Scales

According to algorithms in the previous section, software requires to first determine surface layer similarity scales L and u_*.

The Obukhov length is defined as

$$L = -\frac{u_*^3}{k(g/T_0)(\overline{w'\theta_v'})_s}, \tag{14}$$

in which friction velocity and the surface heat flux can be estimated from measurements of the mean differences or gradients of velocity and temperature between any two heights z_1 and z_2 within the surface layer, but well above the tops of roughness elements.

Letting $\Delta\bar{u} = \bar{u}_2 - \bar{u}_1$ and $\Delta\bar{\theta}_v = \bar{\theta}_{v2} - \bar{\theta}_{v1}$ be the difference in mean velocities and virtual potential temperatures across the height interval $\Delta z = z_2 - z_1$, one can determine the gradient Richardson number (Ri) at the geometric height $z_m = (z_1 z_2)^{1/2}$ by

$$Ri(z_m) = \frac{g}{T_0} z_m \left(ln\frac{z_2}{z_1}\right) \frac{\Delta\bar{\theta}_v}{(\Delta\bar{u})^2}. \tag{15}$$

The corresponding value of the Monin-Obukhov stability parameter $\zeta_m = z_m/L$ can be determined from the relations given by (Arya, 1988)

$$\zeta_m = Ri(z_m), \quad \text{for} \quad Ri < 0, \tag{16}$$

$$\zeta_m = \frac{Ri(z_m)}{1 - 5Ri(z_m)}, \quad \text{for} \quad 0 \leq Ri < 0.2. \tag{17}$$

Then, the basic universal similarity functions ϕ_m and ϕ_h are directly related to ζ_m, i.e.,

$$\phi_h = {\phi_m}^2 = (1 - 15\zeta_m)^{-1/2}, \quad \text{for} \quad \zeta_m < 0 \tag{18}$$

$$\phi_h = \phi_m = (1 + 5\zeta_m), \quad \text{for} \quad \zeta_m \geq 0 \tag{19}$$

The similarity relations of $Eqs.(17)$ and (19) are not valid for $Ri \geq 0.2$ and $\zeta_m > 1$.

Finally, the friction velocity and the surface heat flux can be obtained from the following relations

$$u_* = \frac{k\Delta\bar{u}}{\phi_m(\zeta_m) ln(z_2/z_1)}, \tag{20}$$

$$(\overline{w'\theta_v'})_s = -\left[\frac{k^2 \Delta\bar{u}\Delta\bar{\theta}_v}{\phi_m(\zeta_m)\phi_h(\zeta_m)\left(ln\frac{z_2}{z_1}\right)^2}\right]. \tag{21}$$

The parameters $Ri(z_m)$ and z_m/L are used to determine the stability criteria discussed in the previous section, while the friction velocity u_* is used to estimate the ABL height h in the neutral and stable boundary layer.

3.2 TKE and EDR Profiles in Neutral and Stable Boundary Layer ($z_m/L \geq 0$)

The boundary layer height can be estimated as the minimum of those given by the following diagnostic relations (Arya, 1995):

$$h = 0.3\frac{u_*}{f}, \tag{22}$$

$$h = 0.4\left(\frac{u_* L}{f}\right)^{1/2}, \tag{23}$$

where f is the Coriolis parameter. Note that $Eq.(22)$ is valid only for a stationary neutral boundary layer, but it gives an upper bound for h in slightly stable or near-neutral conditions when L becomes too large and $Eq.(23)$ overestimates h.

Then, $Eqs.(4)$ and (5) are applied to obtain TKE and EDR profiles above $z = 40\,m$ height. The friction velocity in $Eqs.(4)$ and (5) is adjusted so that the profiles are continuous at $z = 40\,m$, and might be slightly different from that given by $Eq.(20)$.

3.3 TKE and EDR Profiles in Unstable Boundary Layer ($z_m/L < 0$)

3.3.1 Strongly Unstable (Convective) Regime ($|z_m/L| > 0.5$)

In this regime, the ABL height is usually estimated from the height of the inversion base, which can be determined from the vertical temperature sounding. However, it is difficult to obtain the temperature inversion base from the existing sounding data from the Dallas/Ft. Worth (DFW) and Memphis field experiments. This is because the soundings often do not extend above a height of $1\,km$, whereas the ABL height in this regime can easily reach a height of $2-3\,km$. Alternatively, we estimate the boundary layer height from $Eqs.(11)$ and (12), using the measured TKE and EDR at $z = 40\,m$, i.e.,

$$h = \frac{0.4 + \sqrt{0.16 + 0.3\, z_{40}\, \epsilon_{40}/(e_{40}/0.54)^{1.5}}}{\epsilon_{40}/(e_{40}/0.54)^{1.5}}, \tag{24}$$

where subscript 40 represents $z = 40\,m$. Although the height of $z = 40\,m$ is within the surface layer ($z \leq 0.1h$) in most of cases of this regime, the observations indicate that the

mixed layer similarity may also be used for the entire boundary layer except for the layer very close to the surface.

Then, *Eqs.*(10) and (12) are applied to obtain TKE and EDR profiles above $z = 40\,m$ height, respectively. The convective velocity scale in *Eq.*(10) is adjusted for the TKE profile to be continuous at $z = 40\,m$, and will be slightly different from that estimated from *Eq.*(11).

3.3.2 Moderately Unstable Regime ($0.02 < |z_m/L| \leq 0.5$)

This regime also includes the cases of $e_5 > e_{40}$ but $|z_m/L| > 0.5$, since TKE (i.e., e) usually increases with height near the surface in the convective regime. The profiles are obtained in the same way as in the convective regime except that *Eq.*(11) is used for TKE profile rather than *Eq.*(10).

3.3.3 Weakly Unstable (Near-Neutral) Regime ($|z_m/L| \leq 0.02$ or $|h/L| \leq 1.5$)

In this regime, the formulations for the neutral boundary layer are applied for the profiles.

4 Comparisons with Observed Data

The friction velocity and TKE and EDR at $z = 5\,m$ and $40\,m$ estimated from the similarity relations in the previous sections have been compared to measurement data from the Dallas/Ft. Worth (DFW) Airport Field Experiment (Dasey et al., 1998) during the period of September 15 - October 3, 1997. The height of $z = 5\,m$ is essentially assumed to be within the surface layer. The measured u_* and EDR are 30-minute averaged, while the measured TKE is a median value over 30-minutes. The frequency for each stability regime is shown in Table 1, indicating that most of data belong to stable and moderately unstable regimes. In the following, the comparisons are performed in two stability groups, that is, neutral and stable regime including the weakly unstable regime and unstable regime including moderately unstable and convective regimes.

4.1 Friction Velocity (u_*)

Figure 1 shows that the estimated u_* from mean velocity measurements with *Eq.* (20) agrees well with the measured u_* from the momentum flux at $z = 5\,m$, but the data scatter becomes larger for weaker u_*. In particular, for very small values of u_*, which are often obtained during very stable conditions, the estimated u_* tends to be significantly smaller than the measured u_*. This is because the Monin-Obukhov similarity theory on which u_* estimates are based, is not applicable under very stable conditions (Nappo and Johansson, 1999).

4.2 TKE at $z = 5\,m$ and $40\,m$

As formulated in sections 2 and 3, the estimated TKE at $z = 5\,m$ in neutral and stable conditions is given as a function of only u_*, while in unstable conditions, it is given as a function of u_*, w_*, L and z. As shown in Fig. 2, the estimated TKE appears to agree with the measured, although data scatter becomes larger for smaller values. This is especially true in neutral and stable conditions. For very small values of TKE, most of the estimated

TKE values are significantly lower than the measured TKE. The agreement between the estimated and measured TKE is much better for the unstable conditions.

At $z = 40\,m$, only a comparison for the neutral and stable conditions is conducted. In unstable conditions, the w_* and h are calculated from the measured EDR and TKE at $z = 40\,m$ and thus, the estimated TKE and EDR at $z = 40\,m$ will match their measured values at $z = 40\,m$, exactly. Figure 3 shows that similar to TKE at $z = 5\,m$, the estimated TKE in neutral and stable conditions agrees reasonably well with the measured TKE, but data scatter at $z = 40\,m$ is larger than that at $z = 5\,m$, especially for smaller TKE values.

4.3 EDR at $z = 5\,m$ and $40\,m$

Using the estimated values of u_* and L, EDR at $z = 5\,m$ is calculated from *Eqs.* (2) and (9). Its 'measured' values were obtained from the power spectrum of the observed wind data using the theoretical Kolmogorov relations of the spectra in the inertial subrange.

Figure 4 shows that at $z = 5\,m$, the estimated EDR appears to increase linearly with increasing measured EDR, but is considerably overestimated in both stability regimes. Data scatter is somewhat larger compared to that of TKE. Similar to that of TKE, however, the data scatter increases with decreasing values of EDR and is larger in neutral and stable conditions than in unstable conditions. As explained in section 4.2, the comparison for EDR at $z = 40\,m$ is conducted only for the neutral and stable conditions. Figure 5 shows that agreement and data scatter between estimated and measured EDR at $z = 40\,m$ are similar to those at $z = 5\,m$, but with smaller overestimation.

4.4 Adjustments in TKE and EDR Profiles

As shown in the above comparison plots, the ABL similarity theory appears to represent the measured u_* and TKE at $z = 5\,m$ and $z = 40\,m$ reasonably well, but with increasing data scatter for decreasing values of u_* and TKE. On the other hand, the estimated EDR considerably overestimates the measured EDR, although estimated and measured values appear to

be strongly correlated with a linear relationship between the two. As described in section 3, therefore, we require that the generated profiles for TKE and EDR match the measured values at $z = 5$ and $40\,m$ while maintaining the profile shape from the similarity theory above $z = 40\,m$. Otherwise, the estimated profiles for TKE and EDR may significantly deviate from those 'measured', especially for small values of TKE and EDR.

5 Procedure of Running Software

The software is coded in FORTRAN and is designed for operational use. The code is composed of one main program and two subroutines. As input the main program reads data files containing TKE and EDR at $z = 5\,m$ and $z = 40\,m$, as well as mean winds and virtual potential temperatures at two levels near the surface. The subroutine "EDRTKE_STABLE" computes TKE and EDR profiles under neutral and stable conditions. The other subroutine "EDRTKE_UNSTABLE" computes TKE and EDR profiles under unstable conditions. On output, vertical profiles of TKE and EDR are generated from the main program.

In executing the code, one needs to enter the following:

- latitude (degree) of the airport, which is used to calculate the Coriolis parameter f.
- one-minute averaged tower data file for wind and virtual potential temperature at two levels near the surface.
- measured 30-minute averaged EDR data file at $z = 5\,m$.
- measured 30-minute averaged EDR data file at $z = 40\,m$.
- measured 5-minute averaged TKE data file at $z = 5\,m$.
- measured 5-minute averaged TKE data file at $z = 40\,m$.

Once the input data files have been successfully entered, the code then generates an output file, which contains not only the vertical profiles of TKE and EDR, but also the output of similarity scales such as h, L, u_*, and w_*. Figures 6 and 7 show a diurnal variation of TKE and EDR profiles generated by the software for a typical sunny day.

6 Summary and Discussion

Based on the existing similarity theories in the atmospheric surface layer and boundary layer under different stability conditions, the expressions and parameterizations for the vertical profiles of TKE and EDR have been suggested. Compared with observation, theoretically estimated TKE at 5 and 40 m heights above ground appears to agree reasonably well with those observed at the same heights except for the very small values of TKE. However, theoretically estimated EDR at 5 and 40 m heights considerably overestimates the observed EDR with large data scatter, although estimated and measured values appear to be strongly correlated with a linear relationship between the two.

From the ABL similarity relationships and their comparisons with the observations, software has been developed to generate realistic vertical profiles of TKE and EDR. The input parameters for the software are the measured TKE and EDR at the heights of $z = 5$ and 40 m above the ground, and the measured winds and virtual potential temperatures at two levels near the ground from which characteristic similarity scales, such as L and u_*, can be estimated. In the software, to minimize the difference between the similarity relations and observations it has been required that calculated values match the observed values at the heights of 5 and 40 m while maintaining the profile shape from the similarity theory above 40 m. Although the software yields very plausible vertical profiles and their diurnal variations, statistics for the difference between the values estimated from the software and the measured values of TKE and EDR at the heights other than 5 and 40 m has to be obtained for further improvement of the software.

7 Acknowledgments

This work was supported by NASA's Terminal Area Productivity program under Contract # NAS 1-18925 (Cooperative Agreement # NCC-1-188). We are greatly indebted to Mr. Robert E. Robins in the Northwest Research Associates, Inc. (NWRA), who has not only provided useful suggestions but also helped correct some errors in the code by producing a number of plots from the code as part of a cooperative effort between NCSU, NWRA, and NASA LaRC. Special thanks are extended to Mr. Steve Maloney at MIT Lincoln Laboratory, who has also provided useful insights which have helped in defining the current approach. The authors are also greatly appreciative for the reviews and comments by Dr. Fred H. Proctor, Mr. David A. Hinton, and Mr. David W. Hamilton, which were very helpful in improving this manuscript.

8 References

Arya, S. P., 1988: Introduction to Micrometeorology. Academic Press, 307 pp.

Arya, S. P., 1995: Atmospheric Boundary Layer and Its Parameterizations. *Wind Climate in Cities*, Cermak, J. E., Davenport, A. G., Plate, E. J., and Viegas, D. X., Eds., Kluwer Academic Publishing, 41-46.

Arya, S. P., 2000: Atmospheric Boundary Layers and Turbulence. *Mesoscale Atmospheric Dispersion*, Boybeyi, Z., ed., WIT Press, Computational Mechanics Publications. (in press)

Caughey, S. J., Wyngaard, J. C., and Kaimal, J. C., 1979: Turbulence in the Evolving Stable Boundary Layer. *J. Atmos. Sci.*, Vol. 36, 1041-1052.

Dasey, T. J., Cole, R. E., Heinrichs, R. M., Matthews, M. P., and Perras, G. H., 1998: Aircraft Vortex Spacing System (AVOSS) Initial 1997 System Deployment at Dallas/Ft. Worth (DFW) Airport. *Project Report NASA/L-3*, 68 pp.

Deardorff, J. W., 1972: Numerical Investigation of Neutral and Unstable Planetary Boundary Layers. *J. Atmos. Sci.*, Vol. 29, 91-115.

Hinton, D. A., 1995: Aircraft Vortex Spacing System (AVOSS) Conceptual Design. *NASA TM-110184*, 27 pp.

Hinton, D. A., Charnock, J. K., Bagwell, D. R., and Grigsby, D., 1999: NASA Aircraft Vortex Spacing System Development Status. *37th Aerospace Sciences Meeting & Exhibit*, Reno, NV, AIAA-99-0753, 17 pp.

Hogstrom, U., 1996: Review of Some Characteristics of the Atmospheric Surface Layer. *Boundary-Layer Meteorol.*, Vol. 78, 215-246.

Monin, A. S. and Obukhov, A. M., 1954: Basic Laws of Turbulent Mixing in the Atmosphere Near the Ground. *Tr. Akad. Nauk SSSR Geoph. Inst.*, No. 24 (151), 1963-1987.

Nappo, C. J. and Johansson, P. -E., 1999: Summary of the LOVANGER International Workshop on Turbulence and Diffusion in the Stable Planetary Boundary Layer. *Boundary-Layer Meteorol.*, Vol. 90, 345-374.

Perry, R. B., Hinton, D. A., and Stuever, R. A., 1997: NASA Wake Vortex Research for Aircraft Spacing. *35th Aerospace Sciences Meeting & Exhibit*, Reno, NV, AIAA-97-0057, 9 pp.

Rao, K. S. and Nappo, C. J., 1998: Turbulence and Dispersion in the Stable Atmospheric Boundary Layer. *Dynamics of the Atmospheric Flows: Atmospheric Transport and Diffusion Processes*, Singh, M. P. and Raman, S., eds., Computational Mechanics Publications, 39-91.

Robins, R. E., Delisi, D. P., and Greene, G. C., 1998: Development and Validation of a Wake Vortex Prediction Algorithm. *36th Aerospace Sciences Meeting & Exhibit*, Reno, NV, AIAA-98-0665, 10 pp.

Sarpkaya, T., Robins, R. E., and Delisi, D. P., 2000: Wake-Vortex Eddy-Dissipation Model Predictions Compared with Observations. *38th Aerospace Sciences Meeting & Exhibit*, Reno, NV, AIAA-2000-0625, 10 pp.

Sorbjan, Z., 1989: Structure of the Atmospheric Boundary Layer. Prentice Hall, 317 pp.

Stull, R. B., 1988: An Introduction to Boundary Layer Meteorology. Kluwer Academic Publishers, 666 pp.

Stability	Frequency (%)
Stable	54
Weakly Unstable	5
Moderately Unstable	37
Strongly Unstable	4

Table 1: Stability frequency (%) in the Dallas/Ft. Worth (DFW) Airport Field Experiment during the period of September 15 - October 3, 1997, where data from two rainy days and one day for which data are partly missing have been omitted from the total data set.

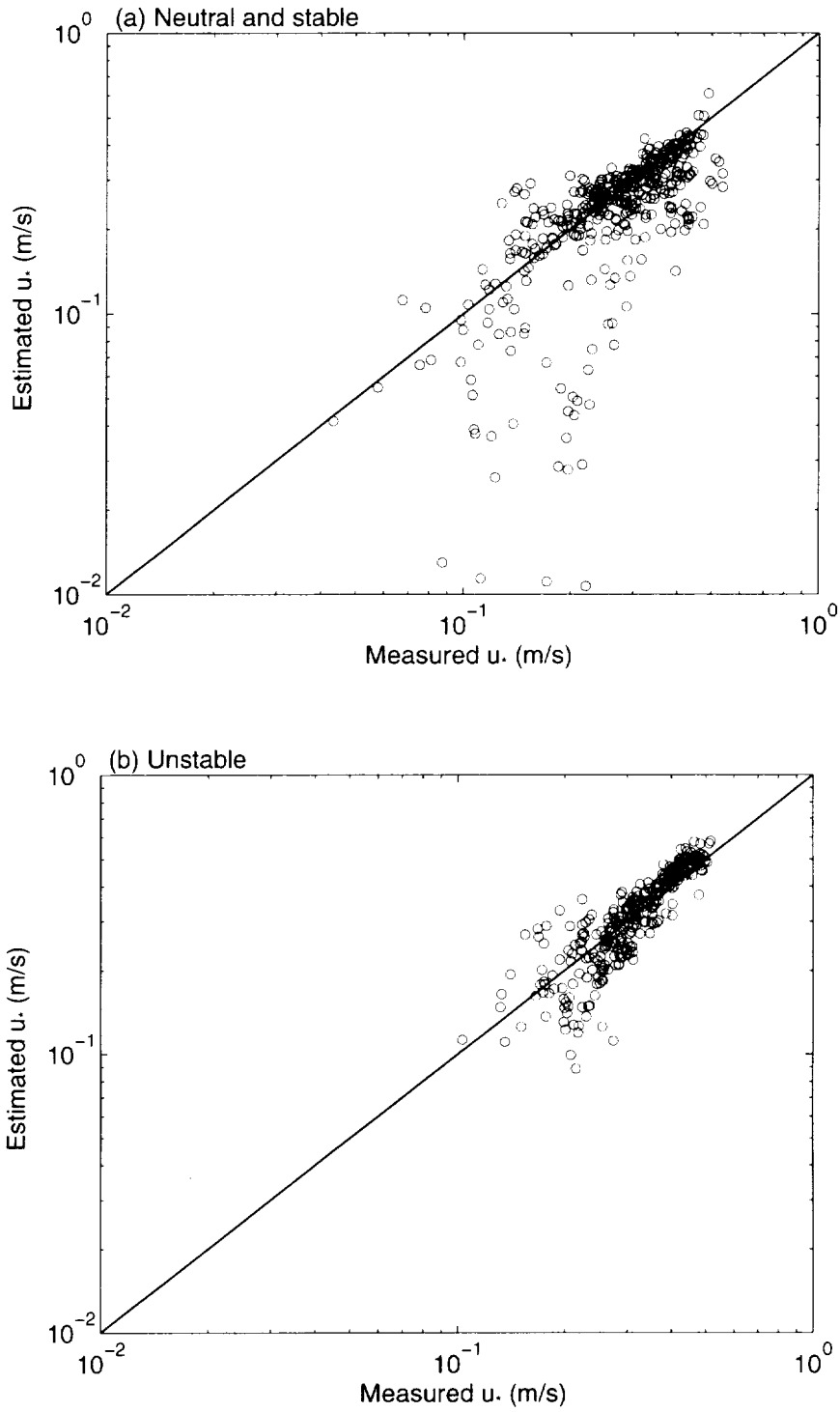

Figure 1: Comparison plots between measured and estimated u_*, where the solid lines represent lines of estimated u_* = measured u_*.

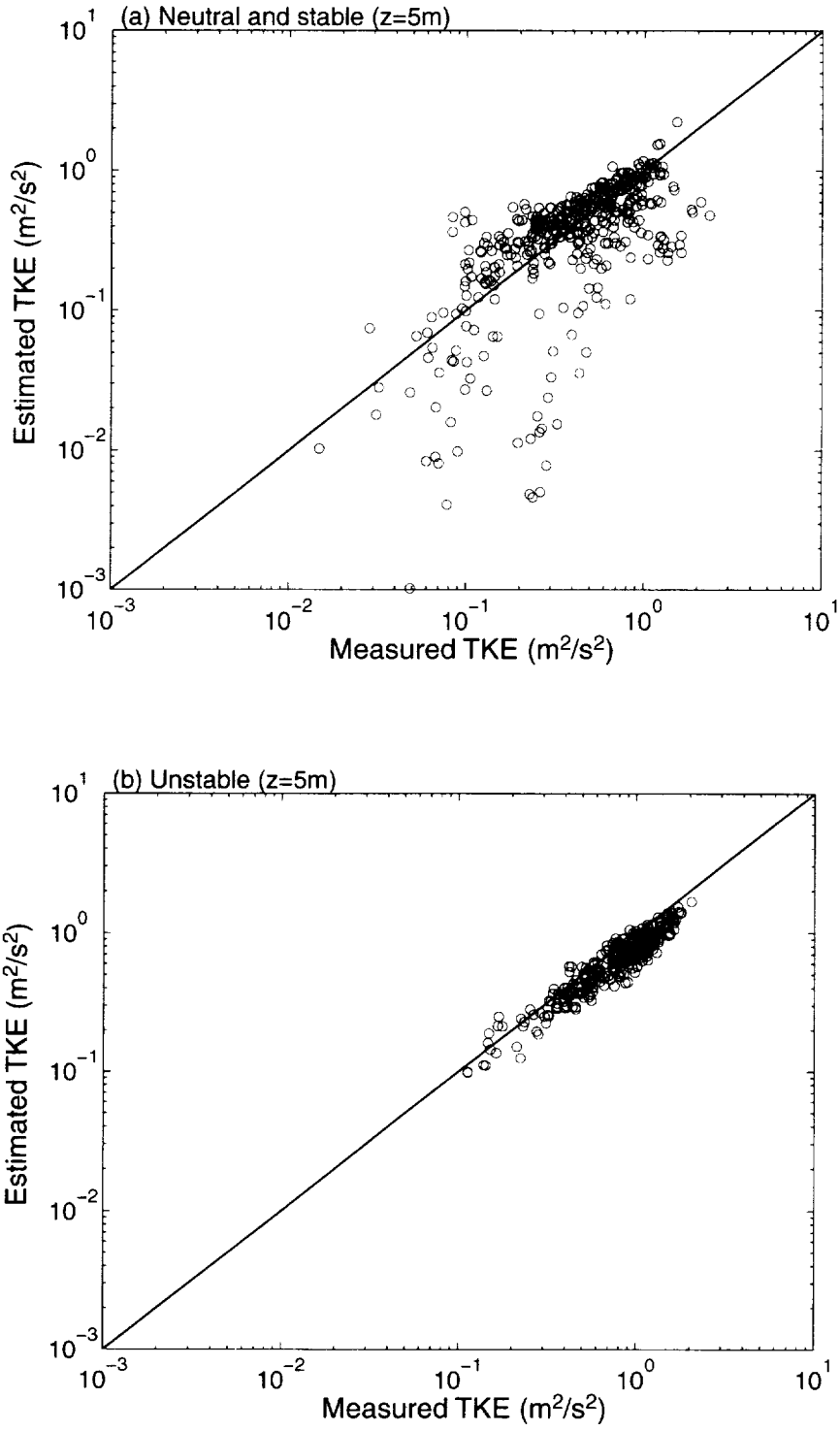

Figure 2: Same as Fig. 1 but for TKE at $z = 5\,m$.

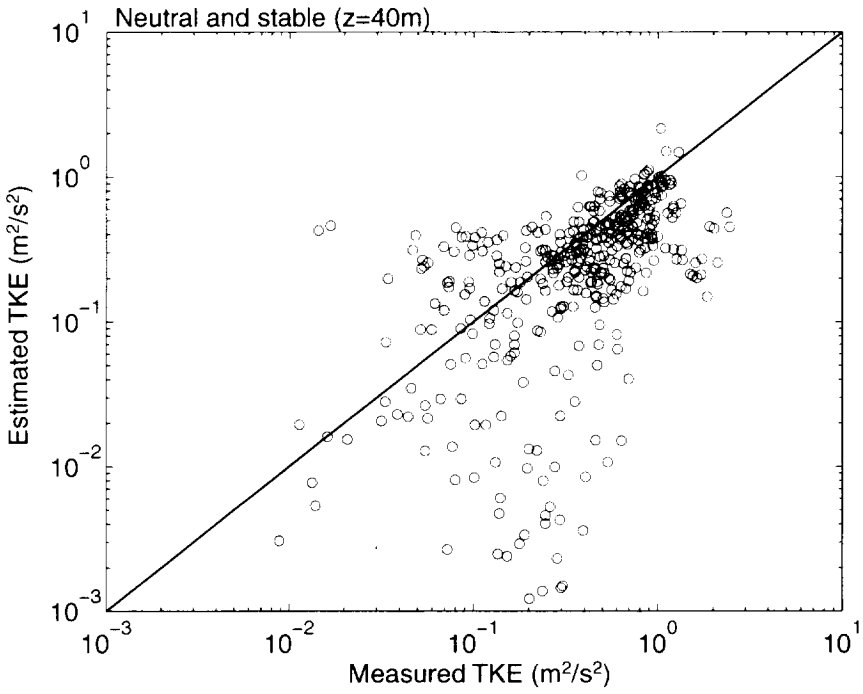

Figure 3: Same as Fig. 1 but for TKE at $z = 40\,m$.

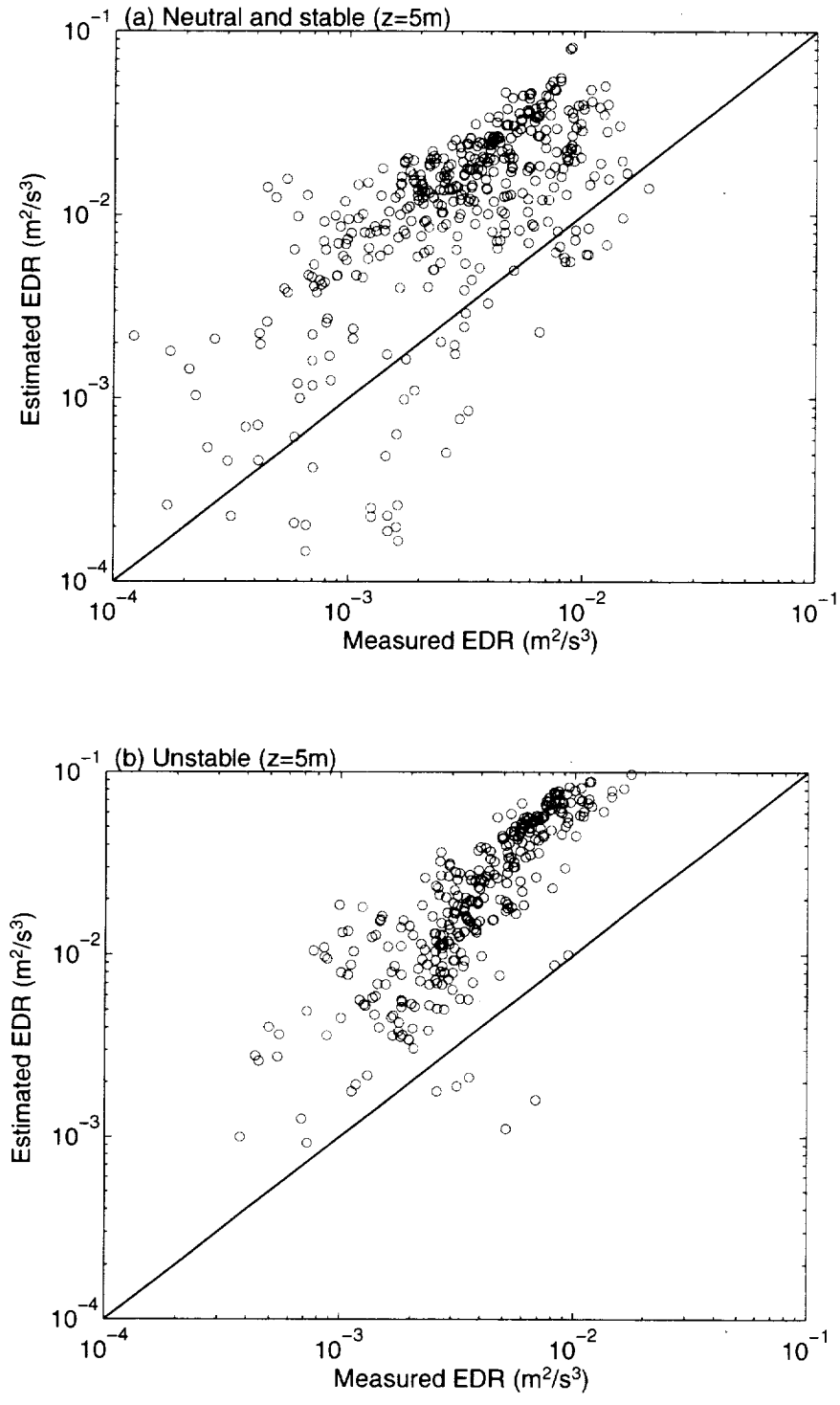

Figure 4: Same as Fig. 1 but for EDR at $z = 5\,m$.

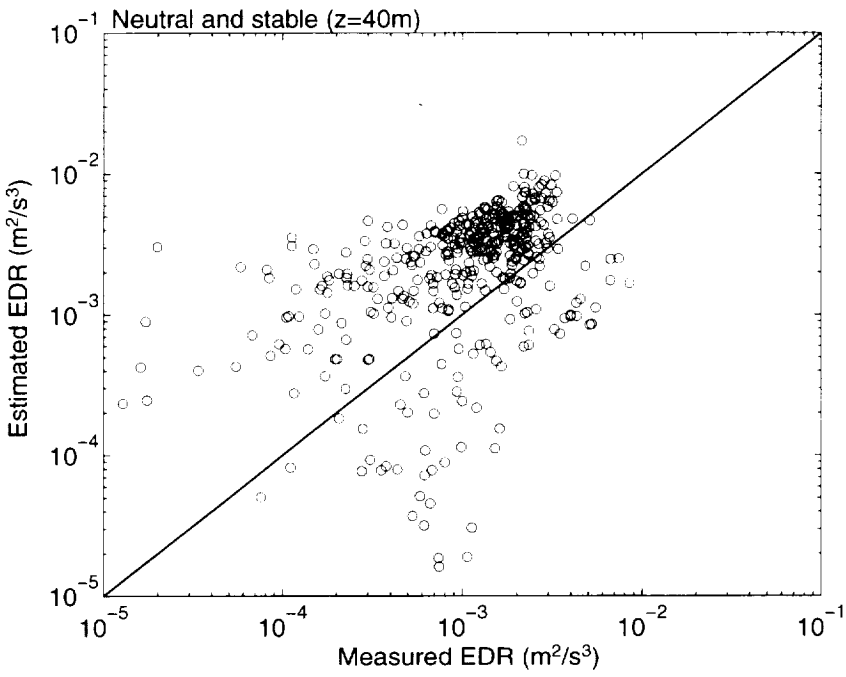

Figure 5: Same as Fig. 1 but for EDR at $z = 40\,m$.

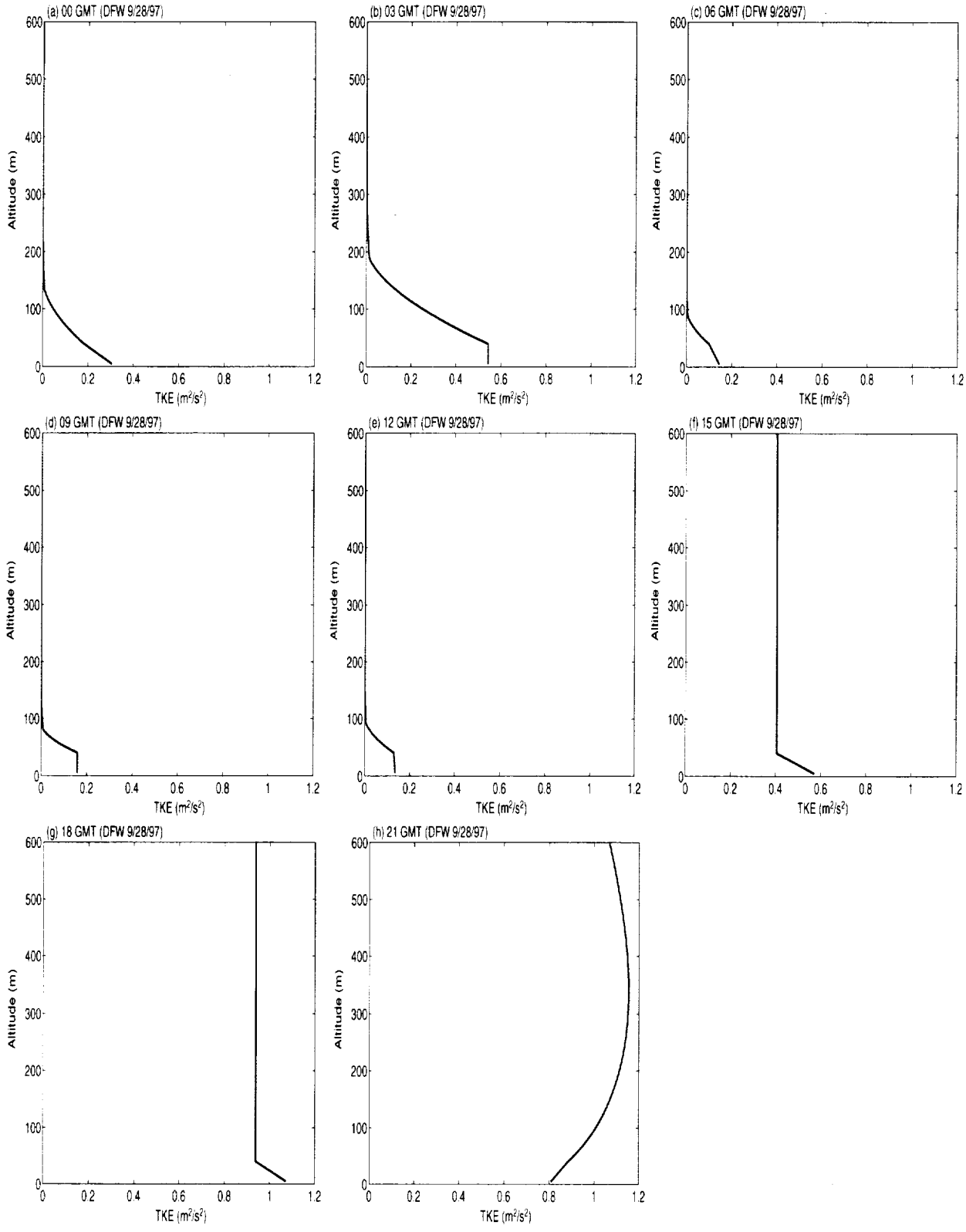

Figure 6: Diurnal variation of TKE profiles obtained from the ABL similarity theory and the observed values of TKE and EDR at $z = 5\,m$ and $40\,m$.

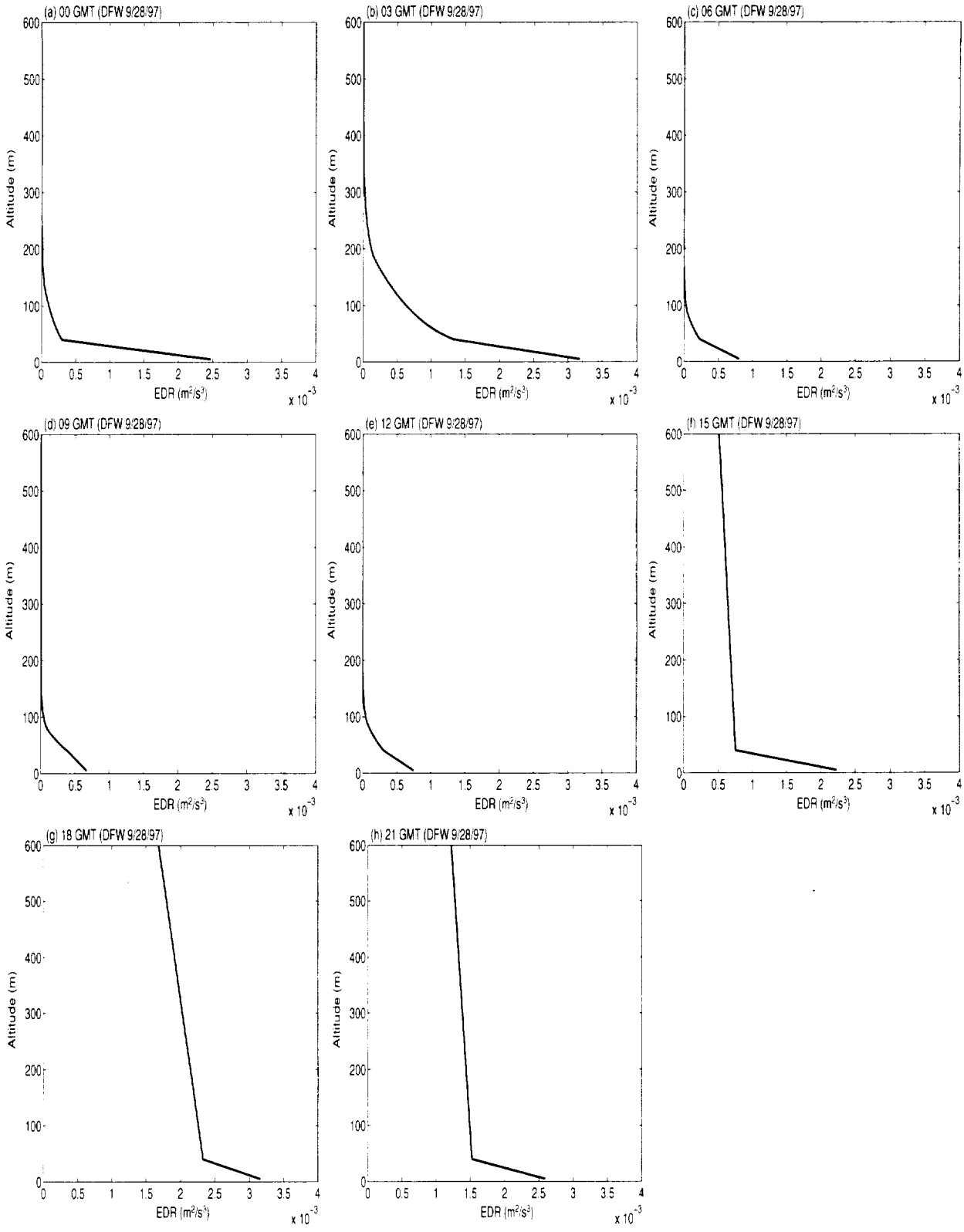

Figure 7: Same as Fig. 8 but for EDR profiles.

REPORT DOCUMENTATION PAGE

Form Approved
OMB No. 0704-0188

1. AGENCY USE ONLY (Leave blank)	2. REPORT DATE	3. REPORT TYPE AND DATES COVERED
	June 2000	Contractor Report

4. TITLE AND SUBTITLE
An Estimation of Turbulent Kinetic Energy and Energy Dissipation Rate Based on Atmospheric Boundary Layer Similarity Theory

5. FUNDING NUMBERS
NCC1-188

576-02-11-11

6. AUTHOR(S)
Jongil Han, S. Pal Arya, Shaohua Shen, and Yuh-Lang Lin

7. PERFORMING ORGANIZATION NAME(S) AND ADDRESS(ES)
North Carolina State University
Department of Marine, Earth and Atmospheric Sciences
Raleigh, NC 27695-8208

8. PERFORMING ORGANIZATION REPORT NUMBER

9. SPONSORING/MONITORING AGENCY NAME(S) AND ADDRESS(ES)
National Aeronautics and Space Administration
Langley Research Center
Hampton, VA 23681-2199

10. SPONSORING/MONITORING AGENCY REPORT NUMBER
NASA/CR-2000-210298

11. SUPPLEMENTARY NOTES
Langley Technical Monitor: Fred H. Proctor

12a. DISTRIBUTION/AVAILABILITY STATEMENT
Unclassified-Unlimited
Subject Category 03 Distribution: Nonstandard
Availability: NASA CASI (301) 621-0390

12b. DISTRIBUTION CODE

13. ABSTRACT (Maximum 200 words)
Algorithms are developed to extract atmospheric boundary layer profiles for turbulence kinetic energy (TKE) and energy dissipation rate (EDR), with data from a meteorological tower as input. The profiles are based on similarity theory and scalings for the atmospheric boundary layer. The calculated profiles of EDR and TKE are required to match the observed values at 5 and 40 m. The algorithms are coded for operational use and yield plausible profiles over the diurnal variation of the atmospheric boundary layer.

14. SUBJECT TERMS
Turbulence Kinetic Energy

15. NUMBER OF PAGES
35

16. PRICE CODE
A03

17. SECURITY CLASSIFICATION OF REPORT	18. SECURITY CLASSIFICATION OF THIS PAGE	19. SECURITY CLASSIFICATION OF ABSTRACT	20. LIMITATION OF ABSTRACT
Unclassified	Unclassified	Unclassified	UL